Estimation of Daily Surface Shortwave Net Radiation From the Combined MODIS Data

Dongdong Wang, Shunlin Liang, *Fellow, IEEE*, Tao He, and Qinqing Shi

***Abstract*—Surface shortwave net radiation (SSNR) is a key component of the surface radiation budget. In this paper, we refined a direct estimation approach to retrieve daily SSNR estimates from combined Terra and Aqua Moderate Resolution Imaging Spectroradiometer (MODIS) data. The retrieved MODIS SSNR estimates were validated against measurements at seven stations of the Surface Radiation Budget Network. We also compared the MODIS retrievals with three existing SSNR products: the Clouds and the Earth's Radiant Energy System (CERES) products, the North American Regional Reanalysis (NARR) data, and the ERA-Interim reanalysis data from the European Centre for Medium-Range Weather Forecasts. MODIS data at 1 km were upscaled to mitigate the mismatch between site measurements and satellite retrievals. Among the four data sets, the aggregated MODIS retrievals agreed best with *in situ* measurements, with a root-mean-square error (rmse) of 23.1 W/m^2 and a negative bias of 6.7 W/m^2. The CERES products have a slightly larger rmse of 24.2 W/m^2 and a positive bias of 7.6 W/m^2. Both reanalysis data (NARR and ERA-Interim) overestimate daily SSNR and have much larger uncertainties. Monthly satellite SSNR data are more accurate than daily values, and the scaling issue in validating monthly MODIS SSNR retrievals is also less prominent. Averaged with a window size of 23 km, the two MODIS sensors can estimate monthly SSNR with an rmse error of 11.6 W/m^2, representing an improvement of 2.4 W/m^2 over the CERES products.**

***Index Terms*—Clouds and the Earth's Radiant Energy System (CERES), ERA-interim, Moderate Resolution Imaging Spectroradiometer (MODIS), North American Regional Reanalysis (NARR), shortwave net radiation, surface radiation budget.**

I. Introduction

SURFACE shortwave net radiation (SSNR), also known as surface-absorbed shortwave radiation, is calculated as the difference between surface downward radiation flux and upward surface radiation flux in the shortwave spectrum (0.3–4.0 μm). SSNR is a dominating factor in the daytime surface radiation budget that is critical to many land surface processes [1] and is strongly correlated with surface all-wave net radiation [2], [3]. Following its definition, an intuitive method for computing SSNR estimates is to first estimate the two components (downward and upward flux) and then calculate the difference between them. Downward shortwave radiation flux can be parameterized using atmospheric variables such as cloud fraction and cloud optical properties [4]. Upward shortwave radiation flux is usually calculated as the product of downward shortwave radiation flux and surface albedo. Hence, both atmospheric and surface parameters are required to compute upward shortwave radiation flux. Surface parameters are also required for some algorithms used to estimate downward shortwave radiation flux, to account for the multiple scattering between the surface and the atmosphere [5]. As a result, this component-based approach involves multiple inputs of surface and atmospheric variables. These input parameters, especially those relating to surface and cloud optical properties, are typically derived from satellite data [6].

An alternative method of calculating SSNR from satellite data is to retrieve it directly from the top-of-atmosphere (TOA) signature received by spaceborne radiometers. Studies have shown that there exists a predictable relationship between surface- and TOA-absorbed shortwave radiation [7], [8]. The relationship is usually modeled as a function of scene type and atmospheric parameters. Earlier studies focused on broadband sensors and used TOA broadband albedo as an input [9]–[11]. Tang *et al.* adapted this approach to multispectral Moderate Resolution Imaging Spectroradiometer (MODIS) data, converting narrowband MODIS TOA reflectances to TOA broadband albedo [12]. Kim and Liang later developed a different scheme for MODIS data and directly estimated SSNR from spectral TOA reflectance [13]. He *et al.* recently refined this approach for the hyperspectral Airborne Visible/Infrared Imaging Spectrometer (AVIRIS) data [14]. Instead of using supplementary water vapor concentrations, He *et al.* estimated this variable from AVIRIS data using a continuum interpolated band ratio algorithm [15].

Since satellite data provide a snapshot of the Earth, the variable derived using the methods described previously typically provides an instantaneous SSNR value. To study the energy balance over time, a temporally averaged or aggregated radiative variable is more needed. Daily radiation can be inferred using interpolation of temporally sparse observations. Direct estimation of SSNR was also initially developed to estimate instantaneous SSNR values. Kim and Liang [13] used a sinusoidal model to infer daily-integrated SSNR from instantaneous values. Wang and Liang [16] recently extended the instantaneous method and applied it to Landsat data to estimate daily SSNR by assuming constant atmospheric conditions during the day. However, the revisiting interval of Landsat data is around two

Manuscript received August 25, 2014; revised January 23, 2015 and February 28, 2015; accepted April 16, 2015.

D. Wang, T. He, and Q. Shi are with the Department of Geographical Sciences, University of Maryland, College Park, MD 20742 USA (e-mail: ddwang@umd.edu).

S. Liang is with the Department of Geographical Sciences, University of Maryland, College Park, MD 20742 USA, and also with the State Key Laboratory of Remote Sensing Science, School of Geography, Beijing Normal University, Beijing 100875, China.

Color versions of one or more of the figures in this paper are available online at http://ieeexplore.ieee.org.

Digital Object Identifier 10.1109/TGRS.2015.2424716

weeks. There are no sufficient Landsat observations to monitor diurnal variability of SSNR. The twin MODIS sensors observe the majority of the Earth at least twice a day, improving models of diurnal changes in SSNR and the accuracy of daily SSNR estimates. Additionally, the Landsat Thematic Mapper (TM) and Enhanced Thematic Mapper Plus (ETM+) do not include absorption bands for water vapor, and supplementary values for total column precipitable water are required to correct the effects of water vapor absorption. In contrast, MODIS has the advantage of including several bands of water vapor absorption in the shortwave infrared spectrum, making it possible to estimate SSNR accurately without supplementary data [17].

In this paper, we refined Wang and Liang's method [16] and applied it to MODIS data to retrieve daily SSNR values without the need for supplementary atmospheric water vapor data. The dependence of regression coefficients on view angles was explicitly considered, and more representative aerosol and cloud types were used to model atmospheric radiative transfer. One year's worth of measurements from seven Surface Radiation Budget Network (SURFRAD) stations was used to validate the retrieved MODIS SSNR data. Additionally, we compared the MODIS results with data from three existing SSNR products from the Clouds and the Earth's Radiant Energy System (CERES), the North American Regional Reanalysis (NARR), and the ERA-Interim reanalysis from the European Centre for Medium-Range Weather Forecasts (ECMWF). The following two sections introduce the data and methodology used in the study. In Section IV, we present and discuss sensitivity analysis, validation results, and data set comparisons, and Section V summarizes the study's findings.

II. Data

A. SURFRAD Measurements

Measurements of surface shortwave radiative fluxes for 2013 at seven SURFRAD sites [18] were used to validate retrievals from MODIS and other existing SSNR data sets. Several variables relating to surface shortwave fluxes are measured at SURFRAD stations using pyrheliometers or pyranometers, including downwelling diffuse solar radiation, downwelling direct solar radiation, downwelling global solar radiation, and upwelling solar radiation, together with their quality information. Since 2001, a new Eppley 8-48 pyranometer has been used to measure downwelling diffuse solar radiation to address cooling issues in the previous instrument [19]. SSNR is calculated as the difference between downwelling global solar radiation and upwelling solar radiation. When good-quality measurements of the two variables are available, the summation of downwelling direct and diffuse solar radiations gives the downwelling global solar radiation. Instruments at SURFRAD stations are calibrated annually, and the uncertainties in direct radiation and diffuse radiation measurements are $\leq 2\%$ and ca. 5%, respectively [20].

B. MODIS Data

The abundance of spectral information from the MODIS makes it possible to obtain information about the surface and the atmosphere simultaneously, through a combination of atmospheric windows and water vapor absorption bands. MODIS data have previously been used to estimate instantaneous SSNR [13], [21]. However, both studies failed to take advantage of MODIS's water vapor channels and required the input of additional water vapor data. TOA reflectance and related geolocation data (MOD02 and MYD02) and cloud mask data (MOD35 and MYD35) from both Terra and Aqua satellites were used in this study. The MODIS data covering the seven SURFRAD sites in 2013 were obtained for algorithm validation. Additionally, MODIS images covering the entire North American continent, acquired on June 9, 2009, were used for data comparison.

C. CERES Products

The CERES is a broadband satellite sensor responsible for several NASA Earth-observing missions, including the Tropical Rainfall Measuring Mission, Aqua, Terra, and Suomi National Polar-orbiting Partnership. The CERES surface radiation budget products incorporate inputs from the CERES broadband instruments, narrowband multispectral radiometers, and other ancillary data sets. Several algorithms were proposed to generate surface shortwave radiation products from CERES data. Level 2 products at the footprint scale use two methods: the direct estimation approach for clear-sky cases [11] and a simple and effective parameterization method for both clear- and cloudy-sky cases [22]. Although level 2 products have higher spatial resolution, they do not provide daily-averaged values. Daily level 3 products are available at an aggregated spatial resolution of 1°, and level 3 surface radiative values are computed using Fu-Liou's [23] radiative transfer codes over 5 atmospheric layers and 15 spectral bands. Albedo is directly estimated from TOA CERES observations [24]. Daily products (SYN1deg_Day) for all-sky surface downward and upward shortwave radiation fluxes for 2013 were also obtained for evaluation.

D. NARR Products

Meteorological data assimilation is another data source for surface radiation variables. Surface shortwave radiation products from the National Centers for Environmental Prediction's (NCEP's) NARR were compared with the MODIS retrievals. Focusing on North America, the NARR has higher spatial resolution (ca. 32 km) than the original NCEP/National Center for Atmospheric Research reanalysis [25]. NARR uses a 3-D variational method to combine observations from various sources (ship and buoy measurements, radiosondes, and satellite radiance) into the NCEP general circulation model (the Eta model), coupled with the Noah land surface model. NARR's albedo input is derived from observed snow cover and climatology data on snow-free and maximum snow albedo.

E. ECMWF ERA-Interim Reanalysis Products

ERA-Interim is a new global meteorological reanalysis project designed to replace the ERA-40 reanalysis [26], with improved representations of the hydrological cycle and

stratospheric circulation [27]. The 3-D variational analysis used for ERA-40 was replaced by 4-D variational assimilation to incorporate the time domain into the objective function [28]. Unlike the NARR data, where users must compute SSNR from surface downward and upward shortwave radiation fluxes, ERA-Interim directly generates SSNR as output. We obtained the ERA-Interim data at a temporal resolution of 3 h and a spatial resolution of 0.75°. Daily SSNR is calculated as the mean of 3-h SSNR data.

III. Modeling Atmospheric Radiative Transfer

This paper presents an approach to directly estimate the daily values of SSNR from MODIS signature. For a given view geometry (Ω), defined as a combination of solar zenith angle (SZA), view zenith angle (VZA), and relative azimuth angle (RAA), daily SSNR $(S_{\text{net}}^{\text{daily}})$ can be calculated from MODIS TOA spectral reflectance (r_b) as follows:

$$S_{\text{net}}^{\text{daily}} = c_0(\Omega, \zeta) + \sum_b c_b(\Omega, \zeta) \cdot r_b \tag{1}$$

where c_0 is the offset and c_b is the coefficient for the band b. The regression coefficients are derived from extensive simulation of atmospheric radiative transfer using representative surface and atmospheric conditions. In addition to view geometry (Ω), the regression coefficients (c) will also be dependent on cloud condition (ζ) (clear or cloudy sky).

Wang and Liang (hereafter WL2014) introduced the idea of estimating daily SSNR from TOA reflectance, using Landsat data as inputs [16]. However, WL2014 used simplified schemes of atmospheric radiative transfer and used only one type of aerosol and cloud for their model. Because of the narrow swath of the Landsat data, WL2014 also used fixed VZA and RAA. Another major improvement in this study is that, unlike WL2014, we do not require supplementary data on atmospheric water vapor to correct our SSNR estimates but make use of a recent study that has suggested the incorporation of MODIS water vapor bands can achieve similar or even better results [17]. In addition to the seven land bands (bands 1–7), water vapor bands of MODIS will be used as well. Different from Landsat TM or ETM+ data, which do not include optical channels of water vapor absorption, MODIS has three water vapor absorption bands (bands 17–19) in the shortwave spectrum. Band 19 of MODIS has the largest bandwidth and is chosen in the study.

MODTRAN5 [29] is used to model atmospheric radiative transfer to obtain a comprehensive database of TOA reflectance and corresponding daily SSNR data for representative surface and atmospheric conditions. To balance between accuracy and efficiency, seven values of SZA, six values of VZA, and seven values of RAA are used to cover a total of 294 cases of view geometry (Table I). MODTRAN is run separately for clear- and cloudy-sky conditions for each of the 294 cases with various inputs of surface and atmospheric parameters. A library of 245 surface spectra from the Advanced Spaceborne Thermal Emission and Reflection Radiometer [30] and the U.S. Geological Survey [31] surface spectra database, covering all major surface cover types, is used as the surface boundary input of MODTRAN.

TABLE I
View Geometry Used in Simulation of Atmospheric Radiative Transfer for Clear- and Cloudy-Sky Conditions

View geometry	Values
Solar zenith angle (SZA)	0°, 10°, 20°, 30°, 45°, 60°, 75°
View zenith angle (VZA)	0°, 10°, 20°, 30°, 45°, 60°
Relative azimuth angle (RAA)	0°, 30°, 60°, 90°, 120°, 150°, 180°

TABLE II
Cloud Base Height (in Kilometers) Used in Simulation of Atmospheric Radiative Transfer for Each Cloud Type

Altostratus	Cumulus	Nimbostratus	Stratus
0.15	0.2	0.15	0.2
1.5	0.6	1.5	0.6
3.0	1.5	3.0	1.0

In terms of atmospheric parameters, the clear-sky simulations mainly consider variations of aerosol and water vapor concentration. Four aerosol types (rural, urban, desert, and biomass burning) are included. For each of the aerosol types, the values of aerosol optical depth can range from 0.0 to 0.4. Six levels of water vapor concentration (0.5, 1.0, 1.5, 3.0, 5.0, and 7.0 g/cm^2) are used. For the cloudy-sky cases, we mainly model the effects of cloud optical properties and atmospheric water vapor. Four types of clouds are currently used, including stratus, cumulus, altostratus, and nimbostratus. Cloud optical depth ranges from 5 to 240, and variations in cloud base height were also considered. Settings for cloud base height differ between cloud types, and three values were used for each type (Table II). Four levels of water vapor concentration (1.5, 3.0, 7.0, and 12.0 g/cm^2) are used for cloudy-sky cases.

MODTRAN can directly produce instantaneous SSNR values $S_{\text{net}}^{\text{inst}}$. To obtain daily SSNR, values of instantaneous SSNR at daytime t are integrated and averaged

$$S_{\text{net}}^{\text{daily}} = \frac{\int S_{\text{net}}^{\text{inst}}(t)\, dt}{T} \tag{2}$$

where T is the length of a day (24 h). For a given combination of surface and atmospheric inputs, $S_{\text{net}}^{\text{inst}}$ is only dependent on SZA. SZA for any daytime t can be easily computed from latitude and solar declination angle. Thus, we are able to obtain data of TOA reflectance and corresponding daily SSNR. With such training data, linear regression is used to get regression coefficients. The coefficients are then saved in look-up tables (LUTs) for future use.

IV. Results and Discussion

A. Sensitivity Analysis

Two groups of regression coefficients, one for clear-sky pixels and the other for cloudy-sky pixels, were used in this study. MODIS cloud mask data were used to select the retrieval path. We used a simple sensitivity analysis to investigate the impact of the reliability of cloud mask data on the accuracy of retrieved SSNR values. The regression coefficients for clear- or cloudy-sky pixels were applied to the simulated observations of the

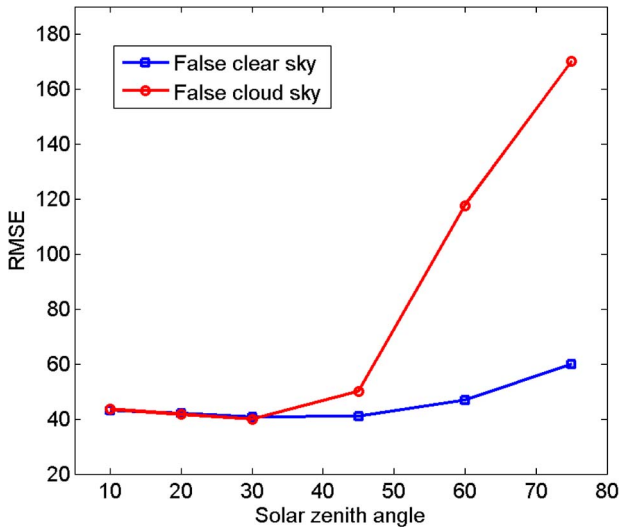

Fig. 1. Sensitivity analysis: impacts of incorrect cloud mask on retrieval accuracy of daily shortwave net radiation.

opposite cloud conditions, and the regressed results were then compared with the simulated SSNR. The results were analyzed according to SZA (Fig. 1). False clear-sky errors, where cloudy-sky pixels are treated as clear-sky pixels, were around 40 W/m^2 and were relatively stable with respect to SZA. For false cloudy-sky observations, the errors were around 40 W/m^2 for data with a small SZA ($\leq 30^\circ$). This value is comparable to the overall error of SSNR estimates (see the following section). However, the errors increased dramatically with SZA. For example, at SZA $= 75^\circ$, the root-mean-square error (rmse) is 180 W/m^2.

In a previous study, one type of aerosol and cloud were used to model atmospheric radiative transfer [16]. To study the impact of aerosol and cloud types on SSNR retrieval, we developed clear-sky coefficients from rural aerosol and cloudy-sky coefficients from stratus cloud only. We then applied these coefficients to different types of aerosol and cloud and analyzed the errors from mismatched aerosol and cloud types (Fig. 2). When the coefficients derived from rural aerosol were applied to the cases of desert aerosol, the resulting errors in SSNR retrievals did not change significantly. However, the errors for the other two aerosol types (urban and biomass burning) were more than doubled. For all aerosol types, errors increased slightly for greater SZA values. Application of the cloudy-sky coefficients showed similar results. Errors were the smallest when applying coefficients to the cloud type used in creating them. The errors caused by underrepresented cloud types were similar for different cloud types with nadir observations. Errors over cumulus and nimbostratus increased significantly for large SZA values. To get presentative coefficients, we used all four aerosol and cloud types to establish the regression coefficients for the final calculation.

B. Validation Results

Using the direct estimation method presented previously, one value of daily SSNR can be estimated for each MODIS observation. For the majority of the Earth's surface, there will be at least two MODIS observations if we combine the Terra and Aqua satellites. Satellite observation frequency is dependent on latitude, and higher latitudes receive more MODIS overpasses. If more than one observation was available for a single day, we averaged the estimates for that day to obtain the final daily SSNR value. We validated the SSNR values retrieved from individual and combined satellites (Table III). A single MODIS sensor is able to retrieve daily SSNR with rmse varying from 25.6 to 46.2 W/m^2 and bias from -19.3 to 4.8 W/m^2 at the seven SURFRAD sites. Analysis of the field measurements suggests that morning SSNR estimates have a stronger correlation with daily SSNR values than the afternoon estimates (Fig. 3). Moreover, morning SSNR values are also a little higher than afternoon values because there are generally fewer clouds in the morning [32]. However, we failed to observe such morning and afternoon difference in the actual satellite retrievals. Aqua results are only marginally worse than Terra results with 1 W/m^2 difference in rmse, since many other factors, such as missing lines in band 6 of Aqua MODIS[33] and the sensor degradation issue in Terra MODIS data [34], complicate the difference between retrievals from the two sensors.

After combining observations from Terra and Aqua, daily SSNR estimates showed a higher correlation with *in situ* data and an rmse reduction of 6–7 W/m^2 compared with estimates based on data from a single MODIS sensor. Results from both MODIS data have a negative bias of -6.7 W/m^2. The combined data underestimate SSNR with a bias of -7.2 W/m^2. Regarding results at individual sites, we saw a bias varying from -16.1 to 2.2 W/m^2. FPK had the smallest rmse (22.0 W/m^2), while the rmse at TBL was the largest (37.4 W/m^2). The mean rmse for all seven sites was 28.7 W/m^2, representing a reduction of 12.3 W/m^2 compared with results from Kim and Liang's earlier study [13]. Wang *et al.* [35] found that the accuracy of daily solar flux values is strongly dependent on the number of daily overpasses. All seven SURFRAD sites are in midlatitudes with an average of 1.8 observations per day. Therefore, it is reasonable to expect higher latitude sites to produce more accurate daily SSNR estimates.

C. Scaling Issue in Validating SSNR Retrievals

Previous studies have found the problem of scaling when validating satellite surface downward solar radiation products [36]. The mismatch between field measurements and satellite products can be attributed to several factors. 1) The spatial coverage of the two types of data is different. Station measurements are point-based and cover a small footprint, while satellite solar radiation products usually have coarse spatial resolution. 2) The field of view for the two types of observations can be different owing to sun-target-sensor geometry. The cloudy-sky pixel on the satellite imagery may actually be sunlit and contribute a high radiation flux value to station measurements. 3) Cloud is a very dynamic phenomenon as its coverage and optical characteristics can change greatly over a short period. To address the issue of spatial scaling, spatial or temporal averaging is commonly used. Gupta *et al.* [22] demonstrated that the correlation between satellite data and *in situ* measurements can be improved by using a temporal mean for *in situ* data

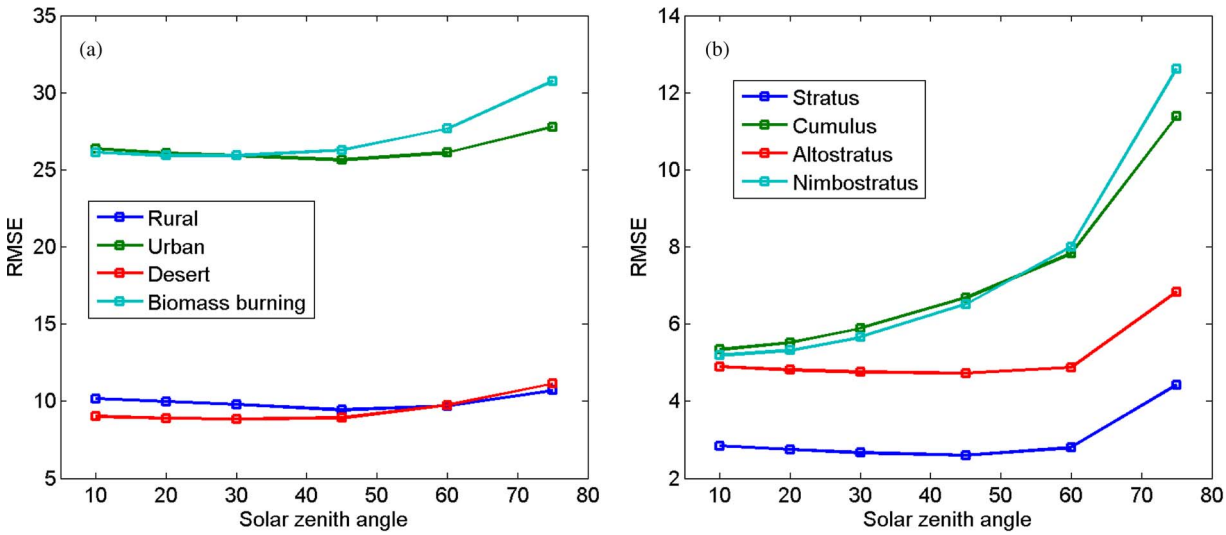

Fig. 2. Impacts of (a) aerosol type and (b) cloud type on retrieval accuracy of daily SSNR.

TABLE III
VALIDATION RESULTS OF DAILY SSNR USING SURFRAD MEASUREMENTS. MODIS DATA ARE FROM THE SINGLE PIXELS CLOSEST TO THE SITES

Sites	Twin			Aqua			Terra		
	R^2	RMSE	Bias	R^2	RMSE	Bias	R^2	RMSE	Bias
Bondville (BND)	0.88	28.0	-0.7	0.82	35.3	-0.6	0.86	31.3	1.7
Fort Peck (FPK)	0.94	22.0	-4.6	0.90	28.9	-3.2	0.86	34.7	-6.3
Goodwin Creek (GCM)	0.88	29.0	-6.5	0.81	37.2	-3.8	0.85	35.9	-9.0
Desert Rock (DRA)	0.92	25.8	-16.1	0.88	32.6	-19.3	0.91	25.6	-12.4
Penn State (PSU)	0.88	27.7	2.2	0.85	32.5	4.8	0.82	36.5	1.4
Sioux Falls (SXF)	0.90	28.8	-10.2	0.86	34.8	-8.5	0.86	34.5	-11.6
Boulder (TBL)	0.83	37.4	-14.5	0.75	46.2	-16.9	0.81	40.6	-11.2
Overall	0.89	28.7	-7.2	0.84	35.6	-6.7	0.85	34.5	-6.7

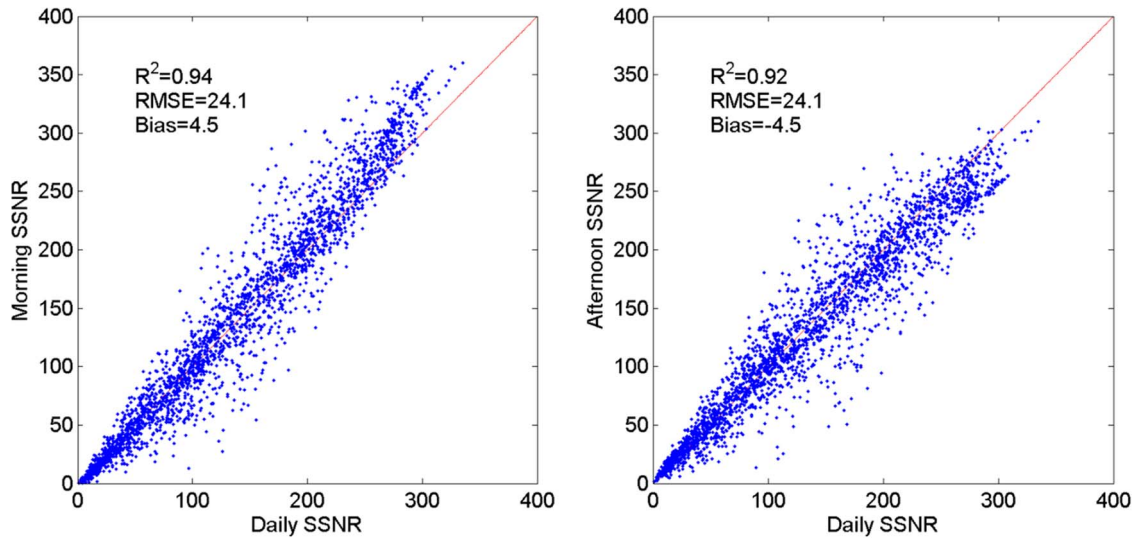

Fig. 3. Comparison of morning and afternoon SSNRs with daily values using the field measurements at seven SURFRAD sites.

around the satellite overpass time, instead of instantaneous measurements at the overpass moment. They concluded that an average over 30–60 min gives the best correlation. Kim and Liang [13] suggested that spatial averaging can also improve this correlation and found that a scale of 9 km resulted in the closest correlations.

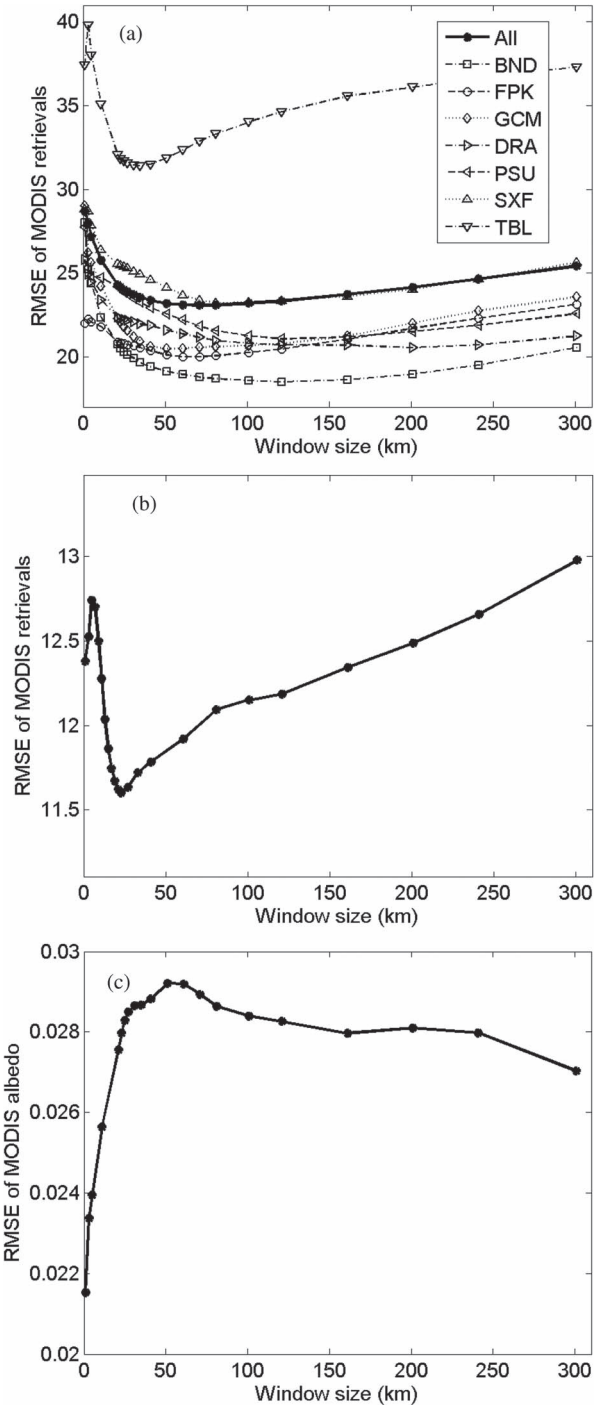

Fig. 4. Impacts of window size on the validation results of satellite radiation quantities. (a) Daily SSNR. (b) Monthly SSNR. (c) Surface albedo.

Since we focused on daily SSNR, temporal averaging of *in situ* data cannot be applied to our validation. We studied the impact of window size of spatial averaging on the agreement between satellite data and *in situ* measurements. Initially, the errors in MODIS retrievals decrease with increasing window size. The errors are smallest when the window size is ca. 70 km [Fig. 4(a)], but any further increase in window size causes larger errors. The optimal window size is also dependent on the temporal resolution of the SSNR data. For the monthly data, the optimal window size was 23 km [Fig. 4(b)]. This is in agreement with a study by Jia *et al.* [37], who found that the accuracy of daily estimates is more sensitive to window size than monthly estimates. Our results also showed that the optimal window size changes from site to site [Fig. 4(a)], with more homogeneous land cover leading to larger optimal window sizes. For example, increasing the window size at the desert site (DRA) to 300 km only increased the retrieval errors by a small amount. Because SSNR is commonly determined by insolation and surface albedo, we also studied the scaling issue for surface albedo data. We considered the difference between SURFRAD measurements and the MODIS albedo product relating to different window sizes and found that albedo errors generally increased with window size [Fig. 4(c)]. Finding the optimal window size is therefore a compromise between decreasing window size to reduce albedo error and slightly increasing window size to reduce errors associated with spatial heterogeneity and cloud dynamics.

D. Data Set Comparison

We also compared daily SSNR products from the CERES, the NARR, and the ERA-Interim reanalysis with SURFRAD measurements. Together with results from MODIS, the results of this comparison are shown in Fig. 5. After increasing window size from 1 to 71 km, errors in MODIS retrieval were reduced by 5.6 W/m^2. The CERES product has a slightly larger rmse of 24.2 W/m^2 and a positive bias of 7.6 W/m^2. The data sets from the two reanalyses are generally of worse quality than the satellite data sets. Both the NARR and ERA-Interim reanalyses substantially overestimate daily SSNR, with positive biases of 30.6 and 7.8 W/m^2, respectively. Among the four data sets, the NARR reanalysis has the lowest quality, with an rmse of 48.4 W/m^2. Previous studies that evaluated downward shortwave radiation products from reanalyses also found substantial overestimations [37]–[39]. Although a small overestimation of 2 W/m^2 can be attributed to code errors in the ERA-Interim reanalysis [27], the major cause of overestimation is the significant underestimation of cloud coverage [40].

We further compared the two satellite data sets (MODIS retrievals and CERES products). The detailed results of this comparison are summarized in Tables IV and V. The daily MODIS SSNR retrievals were generally comparable to the CERES products across all of the SURFRAD sites. For both satellite data sets, the results of clear-sky days are better than the estimates of cloudy-sky data. In terms of relative errors, the difference between the clear-sky data and the cloudy-sky data is even larger. The MODIS results were slightly better for cloudy-sky cases with smaller rmse and bias than the CERES data. We further aggregated the daily SSNR data to provide a monthly resolution (Fig. 6). Unsurprisingly, the biases of the two data sets did not change significantly after temporal aggregation. MODIS data have a negative bias of -7.1 W/m^2, whereas the CERES products overestimate monthly SSNR values by 7.3 W/m^2. Compared with the daily data, errors for both data sets were significantly smaller after monthly aggregation. RMSEs for monthly MODIS SSNR data were as small as 11.6 W/m^2, 2.4 W/m^2 smaller than the error for the CERES data.

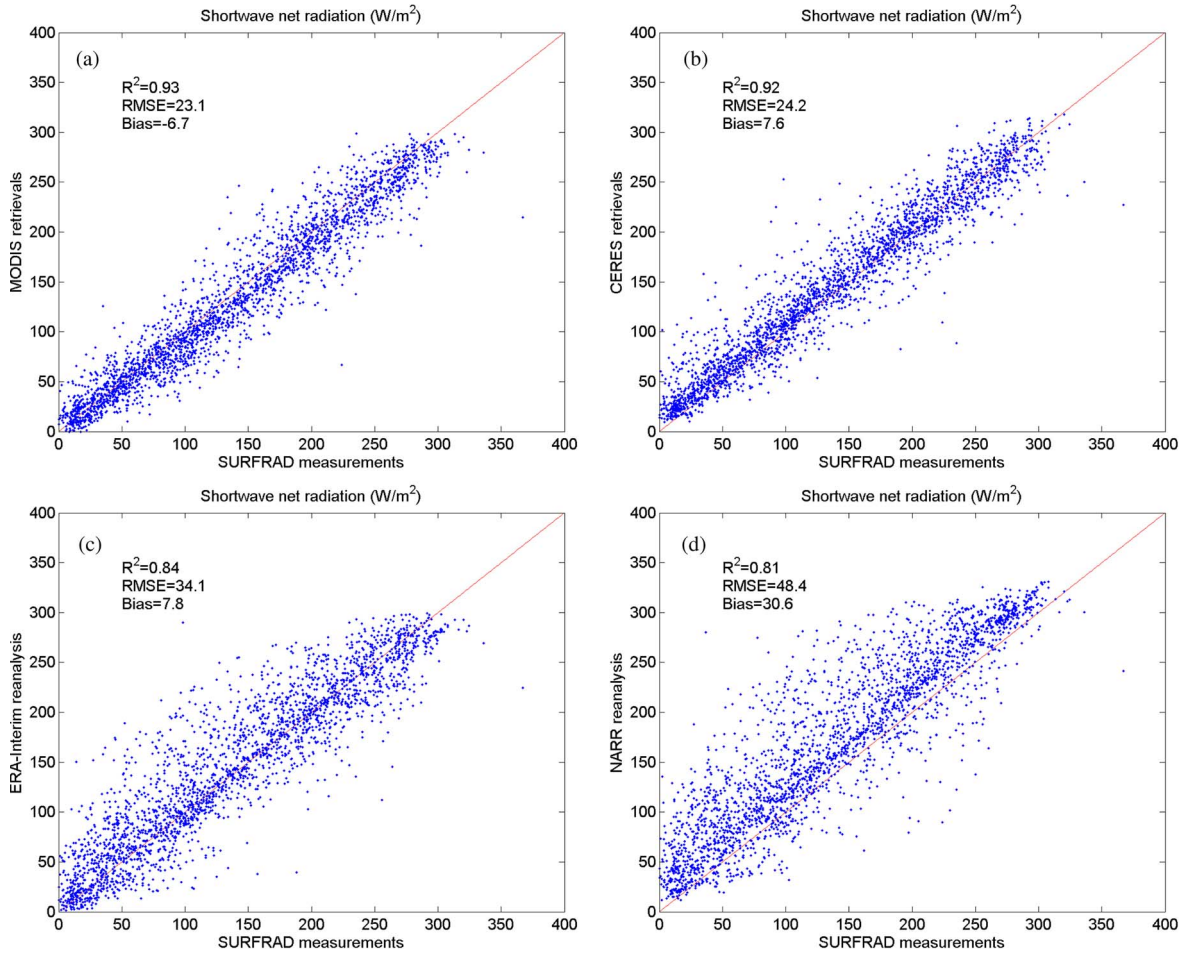

Fig. 5. Comparing field measurements of daily SSNR at seven SURFRAD sites with four data sets. (a) MODIS. (b) CERES. (c) ERA-Interim. (d) NARR. MODIS data are averaged from a 71 km × 71 km window centered at the sites.

TABLE IV
COMPARISON OF VALIDATION RESULTS BETWEEN MODIS AND CERES DAILY SSNR DATA. MODIS DATA ARE AVERAGED FROM A 71 km × 71 km WINDOW CENTERED AT THE SITES

Sites	MODIS Twin			CERES		
	R^2	RMSE	Bias	R^2	RMSE	Bias
BND	0.94	18.8	-1.5	0.94	23.1	13.0
FPK	0.96	20.0	-7.6	0.96	18.1	2.0
GCM	0.94	20.6	-4.5	0.96	18.7	9.7
DRA	0.96	21.1	-14.7	0.96	17.2	-1.2
PSU	0.93	21.8	6.4	0.93	33.5	25.7
SXF	0.93	23.4	-9.1	0.96	17.1	5.5
TBL	0.87	32.9	-15.6	0.81	34.4	-1.7
Overall	0.93	23.1	-6.7	0.92	24.2	7.6

TABLE V
COMPARISON OF VALIDATION RESULTS BETWEEN MODIS AND CERES DAILY SSNR DATA FOR DIFFERENT SKY CONDITIONS. MODIS DATA ARE AVERAGED FROM A 71 km × 71 km WINDOW CENTERED AT THE SITES

Sky condition	MODIS			CERES		
	R^2	RMSE (%)	Bias	R^2	RMSE (%)	Bias
Clear sky	0.93	21.3 (11.3)	-9.4	0.93	20.5 (10.9)	3.4
Cloudy sky	0.92	23.7 (20.1)	-5.6	0.91	25.5 (21.6)	9.2
All sky	0.93	23.1 (16.8)	-6.7	0.92	24.2 (17.6)	7.6

E. SSNR Maps Over North America

We generated a one-day map of SSNR over North America by combining Aqua and Terra data acquired on June 9, 2009, and compared it with maps created from the other three data sets (Fig. 7). SSNR maps from individual MODIS sensors include data gaps at low latitudes due to less frequent coverage. In addition to improved continuity, the combined MODIS map also appears smoother than the single sensor maps. The abrupt boundary due to different satellite orbits is also less evident on the combined map. Owing to the higher spatial resolution, the MODIS map resolves more details than the CERES, the NARR, and the ERA-Interim reanalysis maps. The overall distribution of SSNR data is similar for all four data sets and shows that Greenland has low values due to the high reflectance of snow surfaces, cloud coverage leads to low values over the Great Lakes area, and clear-sky conditions combined with dark surfaces over the west coasts lead to high SSNR values. Discrepancies also exist between the four maps, especially between satellite and reanalysis maps. To quantify the differences, we aggregated MODIS data to match the spatial resolutions of the

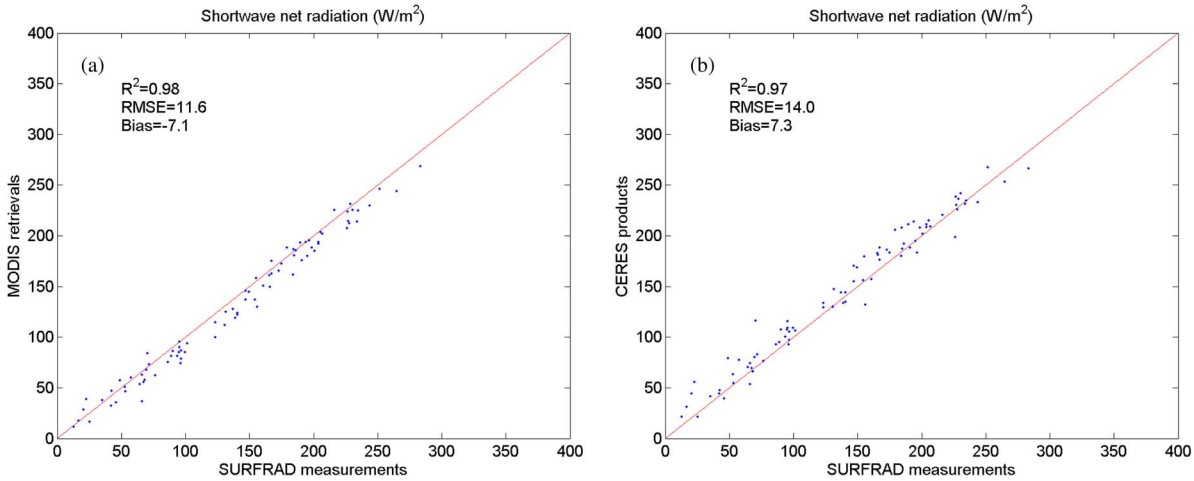

Fig. 6. Comparison of monthly SSNR using SURFRAD measurements with (a) retrievals from the two MODIS sensors and (b) CERES products. MODIS data are averaged from a 23 km × 23 km window centered at the sites.

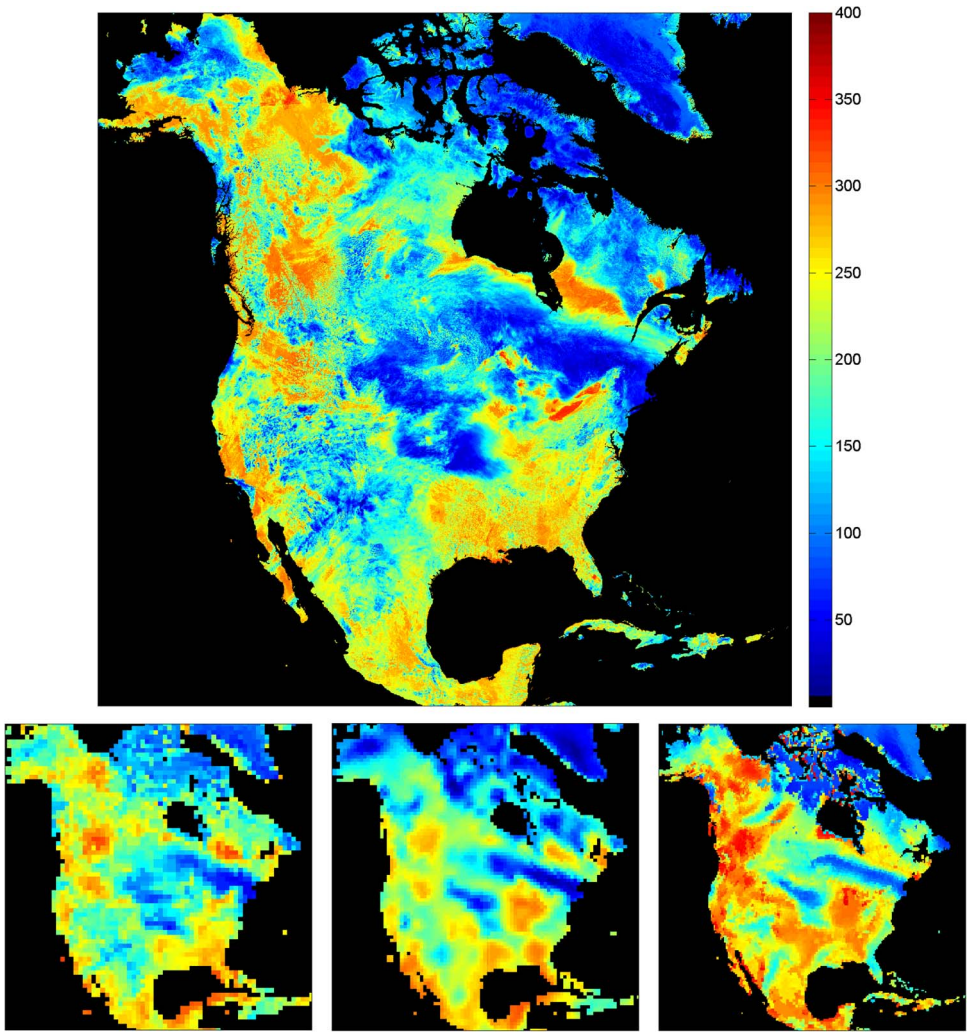

Fig. 7. North American maps of daily SSNR on June 9, 2009, from (a) MODIS, (b) CERES, (c) ERA-Interim, and (d) NARR.

other three data sets and calculated the correlation between them (Fig. 8). CERES data agree reasonably well with MODIS data with R^2 of 0.64 and rmse of 49.4 W/m^2. There also exists systematical difference, and the former is larger than the latter with a bias of 18.3 W/m^2. Among the two reanalysis data, ERA-Interim agrees much better with MODIS results than NARR.

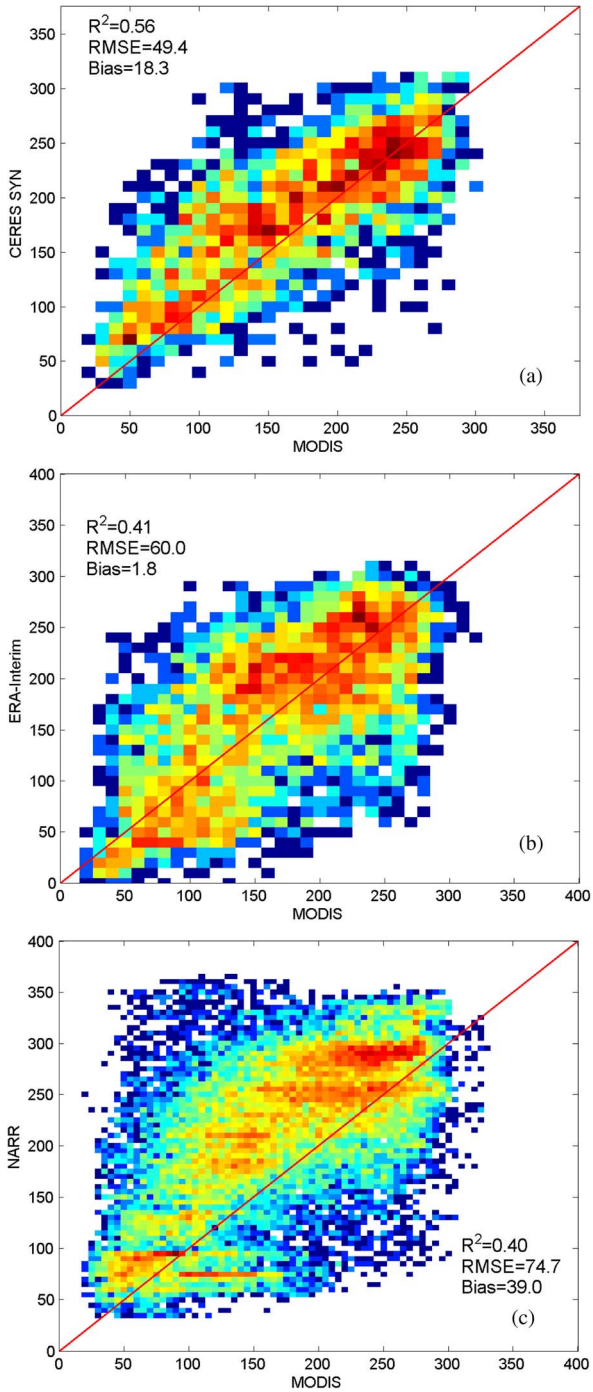

Fig. 8. Scatter plots of daily SSNR between MODIS retrievals and (a) CERES, (b) ECMWF ERA-Interim, and (c) NCEP NARR.

The bias between ERA-Interim and MODIS data is only 1.8 W/m^2. The difference between MODIS and the three other SSNR data shows distinct spatial patterns (Fig. 9). CERES data are generally greater than MODIS estimates, especially over western Alaska and northern Quebec. ERA-Interim data show smaller values in Alaska and northwestern Canada. NARR data are typically much higher than MODIS data in most areas. While the difference maps show no strong dependence cloud coverage and land cover types, further study is needed to understand the cause of such discrepancy.

V. Conclusion

This paper has presented a method for direct estimation of daily SSNR from MODIS TOA reflectance of seven land bands and one water vapor band. The morning Terra MODIS data were combined with the afternoon Aqua MODIS data to improve the mapping of intradaily variations in atmospheric conditions. The synergy of the two MODIS sensors reduced the errors in daily SSNR estimates by 6–7 W/m^2. The mismatch between MODIS estimates and SURFRAD measurements due to the scaling issues can be reduced by spatial upscaling of daily SSNR data. The optimal window size (i.e., that which produces the smallest error) is dependent on several factors and varies from site to site. A value of 71 km was used for validating daily SSNR at the seven SURFRAD sites, and this reduced errors in MODIS estimates by 5.6 W/m^2 (RMSE $= 23.1$ W/m^2 and bias $= -6.7$ W/m^2), a slight improvement over the CERES products. The validation of monthly data requires a smaller window size than that used for daily data. Using a 23-km window, MODIS results for monthly SSNR data have an rmse of 11.6 W/m^2.

The presented method relies on cloud mask data to choose the correct retrieval path. The incorrect information of cloud coverage leads to an error of around 40 W/m^2 for false cloud-sky cases with small VZA and false clear-sky cases. The errors increase substantially with SZA under false cloud-sky circumstances. Two generic LUTs are currently used for all clear- and cloud-sky conditions no matter what aerosol or cloud type is. This paper has analyzed the impacts of aerosol and cloud types on retrieval accuracy. The estimation errors are dependent more on the aerosol type than the cloud type. It could cause errors of greater than 25 W/m^2 if the coefficients derived from rural aerosol were applied over the cases of urban aerosol. With the help of aerosol type information, an aerosol-specific LUT can be developed to improve the estimate of clear-sky SSNR in the future.

The dominant factors influencing daily variations in SSNR are cloud fraction, cloud optical properties, aerosol loading, and water vapor content. These parameters can change substantially over the course of a day. Thus, frequent observations are ideal for modeling intradaily changes in SSNR and obtaining accurate estimates of daily SSNR. Combining data from two MODIS sensors allowed us to arrive at highly accurate daily SSNR estimates. The MODIS results are comparable to or slightly better than the CERES products. It should be noted that the CERES employs geostationary satellites to interpolate atmospheric parameters, and our method could be adapted to work with geostationary data, although the accuracy of SSNR data from traditional geostationary optical imagery may be compromised by their limited spectral channels and coarse spatial resolution. Fortunately, new generation geostationary sensors, such as the Spinning Enhanced Visible and Infrared Instrument and the Advanced Baseline Imager (ABI), have greatly improved spatial and spectral resolutions. For example, ABI has a nadir spatial resolution of 1 km and a spectral configuration similar to the MODIS [41]. A combination of polar-orbiting and geostationary data would enable us to further improve the accuracy of high-resolution daily SSNR estimates.

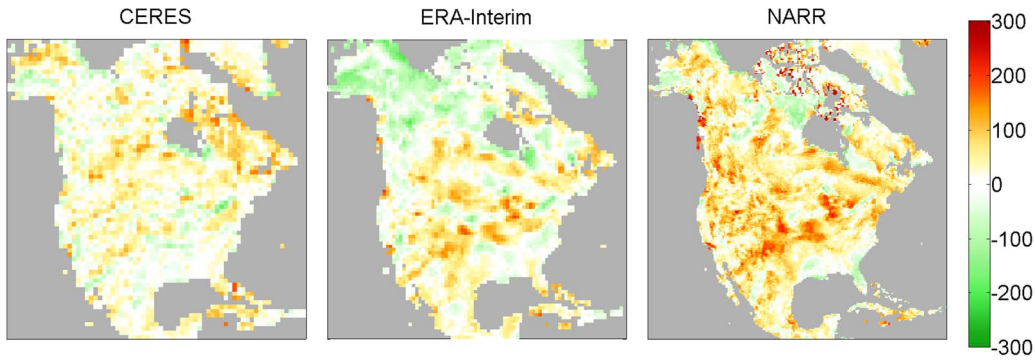

Fig. 9. Spatial distribution of difference between three existing data sets of SSNR and the new MODIS retrievals.

The presented method is an effective tool for mapping daily SSNR from data acquired by multiple spectral radiometers with high spatial resolutions. Due to limited temporal samplings from the two MODIS sensors, we have upscaled the original 1-km data to 71 km to reduce the mismatch between satellite retrievals and field measurements. With the potential addition of geostationary data, we have anticipated providing reliable daily SSNR retrievals at a higher spatial resolution. The generated data can be used as an independent source to evaluate existing products from other satellite sources and different retrieval algorithms and can meet the requirements of some higher resolution applications.

REFERENCES

[1] S. Liang *et al.*, "Review on estimation of land surface radiation and energy budgets from ground measurement, remote sensing and model simulations," *IEEE J. Sel. Topics Appl. Earth Observ. Remote Sens.*, vol. 3, no. 3, pp. 225–240, Sep. 2010.

[2] K. Wang and S. Liang, "Estimation of daytime net radiation from shortwave radiation measurements and meteorological observations," *J. Appl. Meteorol. Climatol.*, vol. 48, no. 3, pp. 634–643, Mar. 2009.

[3] B. Jiang *et al.*, "Empirical estimation of daytime net radiation from shortwave radiation and ancillary information," *Agricult. Forest Meteorol.*, to be published.

[4] G. Bisht *et al.*, "Estimation of the net radiation using MODIS (Moderate Resolution Imaging Spectroradiometer) data for clear sky days," *Remote Sens. Environ.*, vol. 97, no. 1, pp. 52–67, Jul. 2005.

[5] S. Liang *et al.*, "Estimation of incident photosynthetically active radiation from moderate resolution imaging spectrometer data," *J. Geophys. Res.—Atmos.*, vol. 111, Aug. 2006, Art. ID. D15208.

[6] G. Bisht and R. L. Bras, "Estimation of net radiation from the Moderate Resolution Imaging Spectroradiometer over the continental United States," *IEEE Trans. Geosci. Remote Sens.*, vol. 49, no. 6, pp. 2448–2462, Jun. 2011.

[7] R. T. Pinker *et al.*, "The relationship between the planetary and surface net radiation," *J. Clim. Appl. Meteor.*, vol. 24, no. 8, pp. 1262–1268, Aug. 1985.

[8] R. D. Cess and I. L. Vulis, "Inferring surface solar absorption from broadband satellite measurements," *J. Clim.*, vol. 2, no. 9, pp. 974–985, Sep. 1989.

[9] R. D. Cess *et al.*, "Determining surface solar absorption from broadband satellite measurements for clear skies—Comparison with surface measurements," *J. Clim.*, vol. 4, no. 2, pp. 236–247, Feb. 1991.

[10] Z. Q. Li *et al.*, "Surface net solar-radiation estimated from satellite measurements—Comparisons with tower observations," *J. Clim.*, vol. 6, no. 9, pp. 1764–1772, Sep. 1993.

[11] Z. Q. Li *et al.*, "Estimation of SW flux absorbed at the surface from TOA reflected flux," *J. Clim.*, vol. 6, pp. 317–330, Feb. 1993.

[12] B. H. Tang *et al.*, "A direct method for estimating net surface shortwave radiation from MODIS data," *Remote Sens. Environ.*, vol. 103, no. 1, pp. 115–126, Jul. 2006.

[13] H. Y. Kim and S. Liang, "Development of a hybrid method for estimating land surface shortwave net radiation from MODIS data," *Remote Sens. Environ.*, vol. 114, no. 11, pp. 2393–2402, Nov. 2010.

[14] T. He *et al.*, "Estimation of high-resolution land surface net shortwave radiation from AVIRIS data: Algorithm development and preliminary results," *Remote Sens. Environ.*, to be published.

[15] S. Liang and H. Fang, "An improved atmospheric correction algorithm for hyperspectral remotely sensed imagery," *IEEE Geosci. Remote Sens. Lett.*, vol. 1, no. 2, pp. 112–117, Apr. 2004.

[16] D. D. Wang and S. L. Liang, "Mapping high-resolution surface shortwave net radiation from Landsat data," *IEEE Geosci. Remote Sens. Lett.*, vol. 11, no. 2, pp. 459–463, Feb. 2014.

[17] D. Wang *et al.*, "Estimating clear-sky all-wave net radiation from combined visible and shortwave infrared (VSWIR) and thermal infrared (TIR) remote sensing data," *Remote Sens. Environ.*, to be published.

[18] J. A. Augustine *et al.*, "SURFRAD—A national Surface Radiation Budget Network for atmospheric research," *Bull. Amer. Meteorol. Soc.*, vol. 81, no. 10, pp. 2341–2357, Oct. 2000.

[19] J. A. Augustine *et al.*, "An update on SURFRAD—The GCOS Surface Radiation Budget Network for the continental United States," *J. Atmos. Ocean. Technol.*, vol. 22, no. 10, pp. 1460–1472, Oct. 2005.

[20] K. C. Wang *et al.*, "Critical assessment of surface incident solar radiation observations collected by SURFRAD, USCRN and AmeriFlux networks from 1995 to 2011," *J. Geophys. Res.—Atmos.*, vol. 117, Dec. 2012, Art. ID. D23105.

[21] B. Tang and Z. L. Li, "Estimation of instantaneous net surface longwave radiation from MODIS cloud-free data," *Remote Sens. Environ.*, vol. 112, no. 9, pp. 3482–3492, Sep. 2008.

[22] S. K. Gupta *et al.*, "Validation of parameterized algorithms used to derive TRMM-CERES surface radiative fluxes," *J. Atmos. Ocean. Technol.*, vol. 21, no. 5, pp. 742–752, May 2004.

[23] Q. Fu and K. N. Liou, "Parameterization of the radiative properties of cirrus clouds," *J. Atmos. Sci.*, vol. 50, no. 13, pp. 2008–2025, Jul. 1, 1993.

[24] D. Rutan *et al.*, "Development and assessment of broadband surface albedo from Clouds and the Earth's Radiant Energy System clouds and radiation swath data product," *J. Geophys. Res.—Atmos.*, vol. 114, Apr. 30, 2009, Art. ID. D08125.

[25] F. Mesinger *et al.*, "North American Regional Reanalysis," *Bull. Amer. Meteorol. Soc.*, vol. 87, no. 3, pp. 343–360, Mar. 2006.

[26] S. M. Uppala *et al.*, "The ERA-40 re-analysis," *Q. J. R. Meteorol. Soc.*, vol. 131, no. 612, pp. 2961–3012, Oct. 2005.

[27] D. P. Dee *et al.*, "The ERA-Interim reanalysis: Configuration and performance of the data assimilation system," *Q. J. R. Meteorol. Soc.*, vol. 137, no. 656, pp. 553–597, Apr. 2011.

[28] F. Rabier *et al.*, "Extended assimilation and forecast experiments with a four-dimensional variational assimilation system," *Q. J. R. Meteorol. Soc.*, vol. 124, no. 550, pp. 1861–1887, Jul. 1998.

[29] A. Berk *et al.*, "MODTRAN5: A reformulated atmospheric band model with auxiliary species and practical multiple scattering options," in *Proc. SPIE*, 2004, p. 6.

[30] A. M. Baldridge *et al.*, "The ASTER spectral library version 2.0," *Remote Sens. Environ.*, vol. 113, no. 4, pp. 711–715, Apr. 15, 2009.

[31] R. N. Clark *et al.*, "USGS Digital Spectral Library Splib06a," U.S. Geological Survey, Reston, VA, USA, 2007.

[32] M. D. King *et al.*, "Spatial and temporal distribution of clouds observed by MODIS onboard the Terra and Aqua satellites," *IEEE Trans. Geosci. Remote Sens.*, vol. 51, no. 7, pp. 3826–3852, Jul. 2013.

[33] X. X. Xiong *et al.*, "On-orbit calibration and performance of aqua MODIS reflective solar bands," *IEEE Trans. Geosci. Remote Sens.*, vol. 48, no. 1, pp. 535–546, Jan. 2010.
[34] D. D. Wang *et al.*, "Impact of sensor degradation on the MODIS NDVI time series," *Remote Sens. Environ.*, vol. 119, pp. 55–61, Apr. 2012.
[35] D. Wang *et al.*, "Estimation of daily-integrated PAR from sparse satellite observations: Comparison of temporal scaling methods," *Int. J. Remote Sens.*, vol. 31, no. 6, pp. 1661–1677, Feb. 2010.
[36] M. Z. Hakuba *et al.*, "Spatial representativeness of ground-based solar radiation measurements," *J. Geophys. Res.—Atmos.*, vol. 118, pp. 8585–8597, Aug. 16, 2013.
[37] B. H. Jia *et al.*, "Evaluation of satellite and reanalysis products of downward surface solar radiation over East Asia: Spatial and seasonal variations," *J. Geophys. Res.—Atmos.*, vol. 118, pp. 3431–3446, May 2013.
[38] X. A. Xia *et al.*, "Analysis of downwelling surface solar radiation in China from National Centers for Environmental Prediction reanalysis, satellite estimates, and surface observations," *J. Geophys. Res.—Atmos.*, vol. 111, no. D9, May 13, 2006, Art. ID. D09103.
[39] H. Qin *et al.*, "Comparison of downward surface solar radiation derived from GMS5/VISSR and of reanalysis products," *J. Ocean.*, vol. 62, no. 4, pp. 577–586, Aug. 2006.
[40] A. K. Betts *et al.*, "Comparison of ERA40 and NCEP/DOE near-surface data sets with other ISLSCP-II data sets," *J. Geophys. Res.—Atmos.*, vol. 111, no. D22, Aug 19 2006, Art. ID. D22S04.
[41] T. J. Schmit *et al.*, "Introducing the next-generation Advanced Baseline Imager on GOES-R," *Bull. Amer. Meteorol. Soc.*, vol. 86, no. 8, pp. 1079–1096, Aug. 2005.

Dongdong Wang received the B.S. degree in environmental sciences from Peking University, Beijing, China, and the Ph.D. degree in geography from the University of Maryland, College Park, MD, USA.

He is currently a Research Assistant Professor with the Department of Geographical Sciences, University of Maryland. His primary research interest includes remote sensing of surface radiation budget, integration of high-level remote sensing land products, climate change, and terrestrial ecosystem.

Shunlin Liang (M'94–F'13) received the Ph.D. degree from Boston University, Boston, MA, USA.

He is currently a Professor with the Department of Geographical Sciences, University of Maryland, College Park, MD, USA, and the School of Geography, Beijing Normal University, Beijing, China. He has published over 220 SCI indexed journal papers. He is the author of the book *Quantitative Remote Sensing of Land Surfaces* (Wiley, 2004) and is the coauthor of the book *Global LAnd Surface Satellite (GLASS) Products: Algorithms, Validation and Analysis* (Springer, 2013). He edited the book *Advances in Land Remote Sensing: System, Modeling, Inversion and Application* (Springer, 2008) and coedited the books *Advanced Remote Sensing: Terrestrial Information Extraction and Applications* (Academic Press, 2012) and *Land Surface Observation, Modeling, Data Assimilation* (World Scientific, 2013). His main research interests focus on estimation of land surface variables from satellite data, Earth energy balance, and assessment of environmental changes.

Dr. Liang was an Associate Editor of the IEEE TRANSACTIONS ON GEOSCIENCE AND REMOTE SENSING and also a guest editor of several remote-sensing-related journals.

Tao He received the B.E. degree in photogrammetry and remote sensing from Wuhan University, Wuhan, China, and the Ph.D. degree in geography from the University of Maryland, College Park, MD, USA, in 2006 and 2012, respectively.

He is currently a Research Assistant Professor with the Department of Geographical Sciences, University of Maryland. His areas of interest include surface anisotropy and albedo modeling, data fusion of satellite products, and long-term regional and global surface radiation budget analysis.

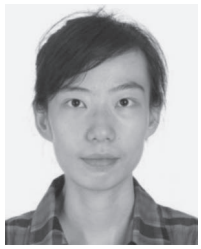

Qinqing Shi received the B.S. degree from the School of Electronics Engineering and Computer Science, Peking University, Beijing, China. She is currently working toward the Ph.D. degree in the Department of Geographical Sciences, University of Maryland, College Park, MD, USA.

She is a Graduate Research Assistant with the Department of Geographical Sciences, University of Maryland. Her research interests include analysis of the surface energy budgets over the Tibetan Plateau and its relationship to the Asian summer monsoon.